

# **Dissipation Wavenumbers for Turbulence in Electron-Positron Plasmas**

S. Peter Gary

Los Alamos National Laboratory, Los Alamos, NM 87545

`pgary@lanl.gov`

Homa Karimabadi

University of California, San Diego, CA 92093

`homakar@gmail.com`

and

Vadim S. Roytershteyn

Los Alamos National Laboratory, Los Alamos, NM 87545

`roytersh@lanl.gov`

Received \_\_\_\_\_; accepted \_\_\_\_\_

Submitted to Astrophysical Journal

## ABSTRACT

**Many astrophysical systems involve turbulent electron-positron plasmas.** Linear kinetic theory of electromagnetic fluctuations in homogeneous, magnetized, collisionless, **non-relativistic** electron-positron plasmas predicts two lightly damped modes propagate at relatively long wavelengths: an Alfvén-like mode with dispersion  $\omega_r = k_{\parallel} \tilde{v}_A$  and a magnetosonic-like mode with dispersion  $\omega_r \simeq k \tilde{v}_A$  if  $\beta_e \ll 1$ . Here  $\tilde{v}_A$  is the Alfvén speed in an electron-positron plasma and  $\parallel$  refers to the direction parallel to the background magnetic field  $\mathbf{B}_o$ . The dissipation wavenumber  $k_d$  is defined as the value of  $k$  at which the damping rate equals the rate of energy transfer by the turbulent cascade. Using linear theory and a basic turbulent cascade model,  $k_d$  is predicted for turbulence at propagation quasi-parallel to  $\mathbf{B}_o$ , for quasi-perpendicular magnetosonic-like turbulence, and for quasi-perpendicular Alfvén-like turbulence. In the latter case, the model predicts that an increase in the turbulent energy should correspond to an increase in  $k_d$ . The assumptions and predictions of the model may be tested by particle-in-cell simulations.

*Subject headings:* turbulence; electron-positron plasmas; dissipation

## 1. Introduction

Electron-positron plasmas constitute important elements of many different astrophysical systems. These include gamma-ray burst sources [(Ramirez-Ruiz et al. 2007; Chang et al. 2008) and references therein], pulsars and their winds (Coroniti 1990; Kazimura et al. 1998), and extragalactic jets [For example, see references in Marscher et al. (2007)]. Although the large-amplitude magnetic fluctuations characteristic of turbulence cannot be directly observed in astrophysical plasmas, *in situ* spacecraft observations have demonstrated that plasma turbulence is ubiquitous throughout the plasmas of the solar wind and observable planetary magnetospheres. Thus it is likely that turbulence will be found in many astrophysical plasmas as well.

The usual picture of turbulence is that it is driven by field perturbations at very long wavelengths, followed by wave-wave interactions which cause the forward cascade of fluctuation energy to successively shorter wavelengths. Finally, at sufficiently short wavelengths, dissipation quenches the cascade and the energy goes into heating of the fluid or plasma. At relatively long wavelengths fluid models such as magnetohydrodynamics (MHD) (Biskamp 2003; Oughton & Matthaeus 2005) or electron magnetohydrodynamics (EMHD) (Biskamp et al. 1999; Dastgeer et al. 2000; Cho & Lazarian 2004) are often used to study the turbulent cascade.

However, as fluctuation wavelengths become shorter, wave-particle interactions in collisionless plasmas generally become stronger, dissipation becomes important, and fluid models fail. As discussed below, if we define the dissipation wavenumber  $k_d$  as marking the onset of significant damping, then at  $k > k_d$  kinetic theories or simulations are necessary to provide a

complete description of turbulence in collisionless plasmas. In particular, kinetic representations are necessary to learn how the energy in turbulent fluctuations is transferred among the various species of a collisionless plasma. Hence, understanding turbulent dissipation is essential for constructing a complete physical picture of how the directed energy in astrophysical jets and flows is converted first to the fluctuating field energy of turbulence and then ultimately to plasma energy.

Particle-in-cell (PIC) simulations, which represent all plasma species as super-particles, offer the potential for fully kinetic solutions to the challenging problem of homogeneous turbulence in collisionless plasmas. Recent PIC simulations have begun to address not only turbulence itself (Gary et al. 2008; Saito et al. 2008), but also its role in astrophysical reconnection (Bessho & Bhattacharjee 2007; Daughton & Karimabadi 2007; Swisdak et al. 2008; Yin et al. 2008) and shocks (Chang et al. 2008).

A second reason to consider electron-positron plasmas is that they facilitate PIC simulation studies of fundamental kinetic processes in collisionless plasmas. Current limitations on the PIC simulation method are not due to any analytic model approximations; rather such computations are constrained by practical limits on particle number, cell size, and computing resources. Because electron-positron PIC calculations are computationally much less demanding than similar calculations in electron-proton plasmas, simulations of the former type can be run to longer times and/or to higher dimensionality than those of the latter. Furthermore, computations of turbulence in electron-positron plasmas, like simulations of whistler turbulence (Gary et al. 2008; Saito et al. 2008), need address only wavelengths which scale with  $c/\omega_e$ , the electron inertial length, and are not required

to embrace the disparate length scales of the electron and proton inertial lengths. Thus electron-positron computations require much smaller system sizes than those needed to capture the full range of kinetic physics in electron-proton plasmas, and can be powerful tools for testing predictions drawn from fundamental theories.

There are two weakly damped electromagnetic modes in homogeneous, magnetized, collisionless electron-positron plasmas: **Alfvén-like fluctuations with dispersion  $\omega_r = k_{\parallel} \tilde{v}_A$  and magnetosonic-like fluctuations with dispersion  $\omega_r \simeq k \tilde{v}_A$  at  $\beta_e \ll 1$** . Here the Alfvén speed in an electron-positron plasma is  $\tilde{v}_A \equiv B_o / \sqrt{8\pi n_e m_e}$  where the subscripts  $e$  and  $p$  refer to electron and positron, respectively. The two modes have identical dispersion at parallel propagation (Iwamoto 1993). In particular both modes have phase speeds  $\omega_r/k$  which monotonically decrease with increasing wavenumber, so that neither mode exhibits whistler-like dispersion with  $\omega \simeq k^2$ .

Using linear kinetic theory and a basic turbulence model, Gary & Karimabadi (2009) predicted certain properties of homogeneous turbulence in electron-positron plasmas. Their predictions include: (i) The forward cascade to shorter wavelengths should preferentially drive fluctuations in directions perpendicular to  $\mathbf{B}_o$ . (ii) Magnetosonic-like turbulence should cascade faster and become more anisotropic than Alfvén-like turbulence. (iii) The anisotropic character of the turbulence implies that both modes should generate modest values of fluctuating electric fields parallel to  $\mathbf{B}_o$ ; it follows, therefore, that these fields should lead to parallel heating of both electrons and positrons.

**This manuscript follows Gary & Karimabadi (2009) in laying the groundwork for computational studies of turbulence in electron-positron plasmas.** We use linear kinetic theory to derive some damping properties of the Alfvén-like and magnetosonic-like fluctuations, and we use these properties in a basic model of cascading plasma turbulence to predict scalings of dissipation wavenumbers of turbulence

at both quasi-parallel ( $k_{\perp} \ll k_{\parallel}$ ) and quasi-perpendicular ( $k_{\parallel} \ll k_{\perp}$ ) propagation.

We denote the  $j$ th species plasma frequency as  $\omega_j \equiv \sqrt{4\pi n_j e_j^2 / m_j}$ , the  $j$ th species cyclotron frequency as  $\Omega_j \equiv e_j B_o / m_j c$ , and  $\beta_{\parallel j} \equiv 8\pi n_j k_B T_{\parallel j} / B_o^2$ . Solutions to the linear dispersion equation are in terms of a wavevector  $\mathbf{k}$  with real components and a complex frequency  $\omega = \omega_r + i\gamma$ . The symbols  $\parallel$  and  $\perp$  denote directions parallel and perpendicular, respectively, to the background magnetic field  $\mathbf{B}_o$ . We define  $\theta$ , the angle of mode propagation, by  $\mathbf{k} \cdot \mathbf{B}_o = k B_o \cos(\theta)$ .

## 2. Linear Theory

This section describes solutions of the linear kinetic dispersion equation for electromagnetic fluctuations in homogeneous, **magnetized**, collisionless, **non-relativistic** electron-positron plasmas. The dimensionless parameters characterizing the zeroth order background plasma are  $\omega_e / |\Omega_e| = 2.5$ ,  $T_e = T_p$ ,  $T_{\perp j} = T_{\parallel j}$ , and  $m_e = m_p$ . Our results are essentially independent of  $\omega_e / |\Omega_e|$  as long as this parameter is much greater than unity. We choose  $\omega_e / |\Omega_e| = 2.5$  for our calculations because PIC simulations run most efficiently when  $\omega_e / |\Omega_e|$  is of order unity. We assume the zeroth order velocity distribution of each species is a Maxwellian, and numerically solve the full electromagnetic dispersion equation (Gary 1993) without analytic approximation.

Linear dispersion properties of the Alfvén-like and magnetosonic-like modes are illustrated in Gary & Karimabadi (2009). **At parallel propagation, the Alfvén-like mode is left-hand circularly polarized, and the magnetosonic-like mode is right-hand circularly polarized.** At  $\mathbf{k} \times \mathbf{B}_o = 0$ , the two modes have identical dispersion and damping (Iwamoto 1993), with essentially zero damping at  $k_{\parallel} c / \omega_e \ll 1$ . At shorter wavelengths, the cyclotron resonances become effective (positron cyclotron resonance for the

Alfvén-like mode and electron cyclotron resonance for the magnetosonic-like mode), causing  $\omega_r$  to become dispersive, and triggering the onset of cyclotron damping. We compute linear damping rates for both modes at  $\mathbf{k} \times \mathbf{B}_o = 0$  and fit the numerical results to the expression

$$\frac{\gamma(k_{\parallel})}{|\Omega_e|} = -m_1 \exp(-4m_2^2 \omega_e^2 / k_{\parallel}^2 c^2) \quad (1)$$

On the domain  $0.01 \leq \beta_e \leq 8$  we obtain

$$m_1 = 0.59 / \beta_e^{0.036}$$

and

$$m_2 = 0.37 / \beta_e^{0.34}$$

As for the case of Alfvén-cyclotron damping in electron-proton plasmas (Gary & Borovsky 2004), this exponential wavenumber dependence of  $\gamma(k_{\parallel})$  represents a prompt onset of cyclotron damping with increasing wavenumber. This stands in contrast to the more gradual, power-law increase in damping due to the Landau resonance at oblique propagation, as illustrated by Equation (2) below.

At propagation oblique to  $\mathbf{B}_o$ , the properties of the two modes diverge; the Alfvén-like mode satisfies  $\omega_r = k_{\parallel} \tilde{v}_A$  at long wavelengths, whereas the magnetosonic-like mode is more nearly isotropic with  $\omega_r \simeq k \tilde{v}_A$  at  $kc/\omega_e \ll 1$  and  $\beta_e \ll 1$ . If  $k_{\perp} \neq 0$ , both modes admit non-zero  $\delta E_{\parallel}$  (Gary & Karimabadi 2009), so Landau damping becomes important. This implies that the damping rate should be proportional to the factor  $\exp(-\omega_r^2 / 2k_{\parallel}^2 v_j^2)$  where  $j$  represents whichever species is Landau resonant with the mode under consideration.

Alfvén-like modes at oblique propagation are analogues of kinetic Alfvén waves in electron-proton plasmas [e.g., Gary & Borovsky (2004, 2008)]. **They may have relatively strong damping at moderately oblique angles of propagation, but, as illustrated in Figure 1, Landau damping approaches zero as  $\mathbf{k}$  approaches the**

**perpendicular.** In the long-wavelength limit, we find that, for  $0.025 \leq \beta_e \leq 8.0$ ,

$$\frac{\gamma}{|\Omega_e|} = -A(\beta_e) \left( \frac{k_{\perp} c}{\omega_e} \right)^2 \frac{|k_{\parallel}| c}{\omega_e} \quad (2)$$

where  $A$  is a monotonically increasing function of  $\beta_e$ , **but is independent of  $\theta$  at least over the range  $60^\circ \leq \theta \leq 85^\circ$ .**

Figure 2 shows  $A(\beta_e)$  which, on the range  $0.04 \leq \beta_e \leq 10.0$ , can be approximately fit by the expression

$$A(\beta_e) \simeq \left( m_1 \beta_e^{1/2} + \frac{m_2}{\beta_e^{5/2}} \right) \exp(-1/2\beta_e)$$

with  $m_1 \simeq 0.23$  and  $m_2 \simeq 0.014$ . The exponential factor of this expression derives from the Landau damping factor  $\exp(-\omega_r^2/2k_{\parallel}^2 v_j^2)$  with  $\omega_r \simeq k_{\parallel} \tilde{v}_A$ .

For magnetosonic-like fluctuations at oblique propagation, we insert the low- $\beta$  dispersion relation  $\omega_r \simeq k \tilde{v}_A$  into the Landau damping factor  $\exp(-\omega_r^2/2k_{\parallel}^2 v_j^2)$  so that

$$\gamma \sim \exp \left( \frac{-1}{2\beta_e \cos^2(\theta)} \right)$$

Using this to guide our analysis, we find that the damping rate of magnetosonic-like fluctuations **in the long-wavelength limit over  $0.05 \leq \beta_e \leq 0.25$  can be fit to the expression**

$$\frac{\gamma}{|\Omega_e|} \simeq -A_{ms}(\beta_e) \left( \frac{kc}{\omega_e} \right) \sin^2(\theta) \exp \left( \frac{-1}{2\beta_e \cos^2(\theta)} \right) \quad (3)$$

**where  $A_{ms}(\beta_e)$  is fully independent of  $\theta$  and is approximately 0.4 for the stated range of  $\beta_e$ . The range of  $\beta_e$  is limited here because our approximation of  $\omega_r = k \tilde{v}_A$  becomes invalid at  $\beta_e \gtrsim 0.25$ , and because the exponential factor makes the damping rate physically insignificant at  $\beta_e \lesssim 0.05$ .**

The  $1/\cos^2(\theta)$  factor in the argument of the exponential is critical; at low  $\beta_e$  the magnetosonic-like fluctuations have very high phase speeds at quasi-perpendicular propagation so that the Landau resonance and its associated damping become very weak.



Figure 1 illustrates this point by plotting the damping rate of the magnetosonic-like mode at long wavelength as a function of  $\theta$ ; although damping is appreciable at  $10^\circ \lesssim \theta \lesssim 35^\circ$ , there is zero damping at both strictly parallel and quasi-perpendicular propagation. Thus for both the Alfvén-like and the magnetosonic-like modes, if wave-wave interactions permit cascades to operate, there are separate channels for those cascades at quasi-parallel and quasi-perpendicular propagation.

Figure 3 illustrates two contours of constant damping rate for each of the two modes. The Alfvén-like contours are similar to the contours for Alfvénic modes in electron-proton plasmas (Gary & Borovsky 2004). At quasi-parallel propagation the contours are closely spaced and essentially vertical, indicating that damping is relatively independent of  $k_\perp$  and that damping has a rapid onset as a function of  $k_\parallel$ , properties which are characteristic of cyclotron damping. At quasi-perpendicular propagation, the contours of the Alfvén-like mode are more widely spaced, consistent with the more gradual wavenumber dependence of Equation (2). The contours of constant damping for the magnetosonic-like mode also exhibit the characteristics of cyclotron damping at quasi-parallel propagation. But for this mode the contour separation remains relatively close as  $\theta$  increases, indicating that the rapid onset of damping with increasing wavenumber persists to quasi-perpendicular propagation.

### 3. Scaling Relations for Turbulence

In this section we use the linear theory results derived in Section II in conjunction with a basic model of the turbulent cascade to derive scaling relations for dissipation wavenumbers of homogeneous turbulence in electron-positron plasmas. We define the

dimensionless energy density of the fluctuating magnetic field,  $\mathcal{E}$ , as

$$\mathcal{E} \equiv \int \frac{|\delta \mathbf{B}(\mathbf{k})|^2}{B_o^2} d\mathbf{k} \quad (4)$$

so that the rate of magnetic energy loss due to damping of fluctuations in a collisionless plasma is

$$\frac{\partial \mathcal{E}}{\partial t} = 2 \int \gamma(\mathbf{k}) \frac{|\delta \mathbf{B}(\mathbf{k})|^2}{B_o^2} d\mathbf{k}$$

where  $\gamma(\mathbf{k})$  is the fluctuation damping rate.

The model which underlies our calculations is as follows. We assume a steady-state condition in which fluctuating energy is imposed on the system at long wavelengths characterized by a wavenumber  $k_o$ , and then cascades through lightly damped modes down to strong dissipation at relatively short wavelengths characterized by a dissipation wavenumber  $k_d$ . We further assume that, if the cascade rate is fast compared to the damping rate, the cascade leads to spectra with power-law dependence on the wavenumber. If, however, damping becomes as fast as the cascade, then, as in Li et al. (2001) power-law spectra can no longer be maintained, and at  $k \gtrsim k_d$  the spectra decrease more rapidly than any power law of the wavenumber.

For example, at quasi-perpendicular propagation we assume the magnetic spectrum can be approximated as

$$\frac{|\delta \mathbf{B}(\mathbf{k})|^2}{B_o^2} = \begin{cases} \epsilon \frac{c^3}{\omega_e^3} \left( \frac{k_{\perp} c}{\omega_e} \right)^{-\alpha} & \text{if } k_o \leq k_{\perp} \leq k_{\perp d} \text{ and } 0 \leq |k_{\parallel}| \leq \Delta k_{\parallel}; \\ 0, & \text{otherwise.} \end{cases} \quad (5)$$

where  $\Delta k_{\parallel} \ll k_{\perp d}$  because the turbulence is quasi-perpendicular. If we use Equation (5) in Equation (4), we obtain

$$\mathcal{E} = 4\pi\epsilon \left( \frac{\Delta k_{\parallel} c}{\omega_e} \right) \int_{k_o}^{k_{\perp d}} \left( \frac{k_{\perp} c}{\omega_e} \right)^{1-\alpha} d \left( \frac{k_{\perp} c}{\omega_e} \right) \quad (6)$$

Our model is based upon the injection of fluctuating magnetic energy at long wavelengths of scale  $2\pi/k_o$ , so physically we expect the contribution from the  $k_o$  term to dominate the

integrand, implying that  $\alpha > 2$  and

$$\epsilon \simeq \frac{(\alpha - 2)\mathcal{E}}{\pi} \left( \frac{\Delta k_{\parallel} c}{\omega_e} \right)^{-1} \left( \frac{k_{\perp} c}{\omega_e} \right)^{\alpha-2} \quad (7)$$

Based upon our linear theory results, we assume that turbulence in homogeneous electron-positron plasmas may be separated into three categories: (a) all modes at quasi-parallel propagation, (b) magnetosonic-like turbulence at quasi-perpendicular propagation, and (c) Alfvén-like turbulence at quasi-perpendicular propagation. We further assume that the ensembles of turbulent fluctuations in each of these three categories are only weakly coupled and that they may be analyzed as if they were independent of each other.

Consider quasi-perpendicular Alfvén-like turbulence with damping as given by Equation (2). We suppose the fluctuating field spectrum is given by Equation (5), and it follows that

$$\frac{\partial \mathcal{E}}{\partial t} = -4\pi A(\beta_e) |\Omega_e| \epsilon \left( \frac{\Delta k_{\parallel} c}{\omega_e} \right)^2 \int_{k_o}^{k_{\perp d}} \left( \frac{k_{\perp} c}{\omega_e} \right)^{3-\alpha} d \left( \frac{k_{\perp} c}{\omega_e} \right) \quad (8)$$

Then, to fulfill the scenario of a forward cascade toward increasing dissipation, the integrand must be an increasing function of  $k_{\perp}$  so that  $\alpha < 3$ .

Thus, in this model, we conclude that power spectra of Alfvén-like turbulence at quasi-perpendicular propagation should satisfy  $2 < \alpha < 3$ . For simulations in a two-dimensional system in which  $k_{\perp}$  corresponds to a single Cartesian coordinate, this condition becomes  $1 < \alpha < 2$ .

At quasi-parallel propagation, and for magnetosonic-like fluctuations at quasi-perpendicular propagation, we find no similar upper bounds on the spectral power law  $\alpha$ . This is because the damping rate is essentially zero at long wavelengths in these two cases, and there is essentially no dissipation until  $k \gtrsim k_d$ .

Collisionless damping typically increases with increasing wavenumber, as in Figure 3, so in our model we assume that changes in the spectral properties occur at wavenumbers

corresponding to the condition of strong damping:

$$\gamma(k) \simeq \left( \frac{1}{\tau_{cascade}} \right) \quad (9)$$

where  $\tau_{cascade}$  is the inverse rate of fluctuating magnetic energy transfer in the turbulent cascade; in general this quantity is a function of plasma parameters as well as the turbulence parameters  $\mathbf{k}$  and  $|\delta\mathbf{B}|^2/B_o^2$ . Equation (9) defines the dissipation wavenumbers  $k_d$  which should be different for each of the three categories.

Consider category (a): both modes at quasi-parallel propagation. As discussed above, damping at  $\mathbf{k} \times \mathbf{B}_o = 0$  is essentially zero at  $k_{\parallel}c/\omega_e \ll 1$ , but then becomes appreciable with a relatively small further increase in the parallel wavenumber. This implies that  $k_{\parallel d}$  should be essentially independent of the amplitude of the turbulent fluctuations and the wavenumber properties of the spectrum, but may be derived directly by considering variations in  $\gamma/|\Omega_e|$  and  $\beta_e$  in linear dispersion theory. Figure 4 illustrates  $k_{\parallel d}$  for both modes as a function of  $\beta_e$  for two values of the damping rate. These results are similar to those for the parallel dissipation wavenumber for Alfvén-cyclotron fluctuations [Fig. 3 of (Gary & Borovsky 2004)]; for the parameters shown here the approximate scaling is

$$k_{\parallel d}c/\omega_e \simeq 0.3/\beta_e^{1/3} \quad (10)$$

or  $k_{\parallel d}v_e/|\Omega_e| \simeq 0.22\beta_e^{0.15}$ .

For category (b), magnetosonic-like fluctuations at quasi-perpendicular propagation, a similar argument for the dissipation wavenumber applies, although it must be extended to two-dimensional wavevectors. The linear theory results of Section II and (Gary & Karimabadi 2009) for this mode demonstrate that for sufficiently large values of  $\theta$  and  $kc/\omega_e$  not too large,  $\gamma \simeq 0$ . However, as for cyclotron damping at parallel propagation, a relatively small increase in  $k$  at fixed  $\theta$  yields a sudden onset of damping. Thus, as we argued for modes at parallel propagation, the spectral breakpoint should be relatively

independent of the properties of the spectrum, and  $k_{\perp d}$  should follow from the choice of  $\gamma/|\Omega_e|$ ,  $\beta_e$ , and  $\theta$  in linear dispersion theory. So, if we consider only  $k_{\perp}c/\omega_e \geq 1.0$  for the two magnetosonic-like threshold curves in Figure 3, we find fits of the form

$$k_{\perp d}c/\omega_e = m_1 \exp\left(\frac{-m_2 k_{\perp d}c/\omega_e}{\tan(\theta)}\right) \quad (11)$$

with  $m_1 \simeq 3$  and  $m_2 \simeq 2.1$  for the two values of  $\gamma/|\Omega_e|$  illustrated there. More generally, these two fitting parameters are functions not only of the dimensionless damping rate, but also depend upon  $\beta_e$ . If simulations of turbulence demonstrate that Equation (11) provides useful insight into quasi-perpendicular magnetosonic-like turbulence, quantification of these parametric dependences would be a worthwhile exercise.

Qualitatively, as the angle of propagation for magnetosonic-like turbulence approaches the perpendicular, the dissipation wavenumber  $k_{\perp d}$  becomes larger, but the dissipation-free channel for the turbulent cascade becomes narrower in  $k_{\parallel}$ . In real plasmas this process cannot continue to arbitrarily large  $k_{\perp}c/\omega_e$ , because the gradually diminishing  $k_{\parallel}$  associated with more nearly perpendicular  $\theta$  demands homogeneity on gradually increasing scales parallel to  $\mathbf{B}_o$ . Thus the inevitable inhomogeneities of physical plasmas (or finite system sizes in computational plasmas) will eventually terminate this type of cascade process.

Third, we examine the dissipation wavenumber for category (c): the quasi-perpendicular cascade of Alfvén-like turbulence. As Figure 3 illustrates, the dissipation-free channel for these fluctuations is much narrower than that for quasi-perpendicular magnetosonic-like turbulence. But another difference between the two types of cascade is that the dissipation scale for quasi-perpendicular Alfvén-like turbulence is a function of the energy density  $\mathcal{E}$ . In Equation (9), we use Equation (2) for the damping rate, and Equation (5) of (Gary & Karimabadi 2009) for the cascade rate. Then

$$A(\beta_e) \left(\frac{k_{\perp}c}{\omega_e}\right)^2 \left(\frac{k_{\parallel}c}{\omega_e}\right) \simeq \frac{\sqrt{2}}{2\pi} \left(\frac{k_{\perp}}{k_{\parallel}}\right) \left(\frac{k_{\perp}c}{\omega_e}\right)^3 \frac{|\delta\mathbf{B}(\mathbf{k})|^2}{B_o^2} \left(\frac{\omega_e}{c}\right)^3 \quad (12)$$

If we multiply both sides of Equation (12) by  $k_{\parallel}$ , invoke Equation (5), and integrate over  $k_{\parallel}$ , then

$$\left(\frac{k_{\perp d} c}{\omega_e}\right)^{\alpha-2} \simeq \frac{3\sqrt{2}\epsilon}{2\pi A(\beta_e)} \left(\frac{\Delta k_{\parallel} c}{\omega_e}\right)^{-2}$$

or, using Equation (7),

$$\frac{k_{\perp d}}{k_o} \simeq \left[ \frac{6\sqrt{2}}{(2\pi)^2} \frac{(\alpha-2)\mathcal{E}}{A(\beta_e)} \left(\frac{\Delta k_{\parallel} c}{\omega_e}\right)^{-3} \right]^{1/(\alpha-2)} \quad (13)$$

Equation (13) is physically plausible. It is consistent with our expectation that an increase in the total fluctuating energy density should push the turbulent spectrum to larger values of the dissipation wavenumber. Similarly, the inverse relationship between  $k_{\perp d}$  and  $\Delta k_{\parallel}$  is qualitatively consistent with the linear theory results of Figure 3. Finally, the smaller the system size (i.e., the larger  $k_o$ ), the harder the turbulence is driven, and thus the larger  $k_{\perp d}$  should be, again consistent with Equation (13).

To illustrate, we choose  $\alpha = 8/3$ ,  $\mathcal{E} = 0.10$ ,  $\Delta k_{\parallel} c/\omega_e = 0.30$ , and  $\beta_e = 0.10$  which implies  $A = 0.02$ . Then  $k_{\perp d}/k_o \simeq 137$ . So our model predicts that, for a simulation in which the driving fluctuations have  $k_o c/\omega_e = 0.02$ , the quasi-perpendicular cascade of Alfvén-like turbulence should carry fluctuation energy out to a relatively short wavelength breakpoint at  $k_{\perp d} c/\omega_e \simeq 2.7$ . Note that this predicted penetration of the turbulence to short wavelengths is due to our choice of  $\beta_e \ll 1$ . At  $\beta_e = 1.0$ , if we keep all other parameters the same,  $k_{\perp d}/k_o$  is reduced by more than an order of magnitude, and the turbulence must be driven harder (i.e., a larger value of  $\mathcal{E}$  and/or a larger value of  $k_o c/\omega_e$ ) to enable the turbulence to attain such short wavelengths.

## 4. Conclusions

**In order to establish a theoretical foundation for future particle-in-cell simulations of astrophysical pair plasmas,** we have examined linear kinetic theory for

electromagnetic fluctuations in homogeneous, magnetized, collisionless, **non-relativistic** electron-positron plasmas. We have used the resulting dispersion properties with a basic cascade model to predict dissipation wavenumbers for three categories of turbulence: (a) both types of modes at quasi-parallel propagation, (b) quasi-perpendicular magnetosonic-like turbulence, and (c) quasi-perpendicular Alfvén-like turbulence. For case (a) we predict that the onset of cyclotron dissipation corresponding to a "breakpoint" in reduced spectra should arise at  $k_{\parallel d}c/\omega_e \simeq 0.3/\beta^{1/3}$ , independent of the total energy in the turbulence. For category (b), we found that the dissipation wavenumber  $k_{\perp d}$  is a function of the direction of propagation and scales with  $\theta$  as Equation (11). This result is derived from the linear theory results illustrated in Figure 3 which suggests that the channel for the quasi-perpendicular cascade of magnetosonic-like turbulence may extend to  $k_{\perp}c/\omega_e > 1$ . For case (c), quasi-perpendicular Alfvén-like turbulence, we assume the spectral form of Equation (5) and predict that  $2 < \alpha < 3$  in three-dimensional simulations or  $1 < \alpha < 2$  in two-dimensional computations. We further predict that the dissipation wavenumber corresponding to the breakpoint wavenumber of such turbulence spectra should increase with increasing turbulent energy and should scale approximately as Equation (13).

The results described here have been obtained from theory derived from the non-relativistic Vlasov equation. For strongly relativistic plasmas, we might expect major changes in the physics. But if we assume that relativistic effects are caused by an increase in the plasma temperature, then it is likely that the first physical consequences of such an increase would be associated with the relativistic increase in mass. Noting that our assumption of  $m_e = m_p$  precludes the appearance of any  $m_e/m_p$  factors in our theory, we speculate that scaling relations for weakly relativistic plasmas should not significantly differ from the results described here.

These predictions, and the predictions of Gary & Karimabadi (2009), can be tested by the use of PIC simulations, and we anticipate that such computations will begin soon. Before considering our predictions, however, the simulations should first address the fundamental assumptions of our model; if these are not satisfied, then there is no foundation upon which our predictions may stand. The most important pillars of our model are: (I) the assumption that turbulence can be separated into three, distinct, relatively independent categories, (II) the assumption that each category of turbulence can be represented as an ensemble of weakly interacting modes which are approximately described by linear dispersion theory, (III) the assumption that weakly-damped cascading turbulence corresponds to a magnetic fluctuation spectrum with a power-law wavenumber dependence, and (IV) the assumption that strongly dissipated turbulence corresponds to a magnetic fluctuation spectrum that decreases more rapidly than any power law in wavenumber. We look forward to early PIC simulations of homogeneous turbulence in collisionless electron-positron plasmas. **We further anticipate that these simulations will bring new insights to the study of how such turbulence heats collisionless astrophysical plasmas.**

We acknowledge useful discussions with Joe Borovsky. The Los Alamos portion of this work was performed under the auspices of the U.S. Department of Energy (DOE). It was supported by the Magnetic Turbulence and Kinetic Dissipation Project of the Laboratory Directed Research and Development Program at Los Alamos, and by the Solar and Heliospheric Physics SR&T and the Heliophysics Guest Investigators Programs of the National Aeronautics and Space Administration. Work at UCSD was supported by NSF-GEM grant ATM-0802380.



## REFERENCES

- Bessho, N., and Bhattacharjee, A., 2007, Phys. Plasmas, 14, 056503.
- Biskamp, D., 2003, *Magnetohydrodynamic Turbulence*, Cambridge University Press, New York.
- Biskamp, D., Schwartz, E., Zeiler, A., Celani, A., and Drake, J. F., 1999, Phys. Plasmas, 6, 751.
- Chang, P., Spitkovsky, A., and Arons, J., 2008, ApJ, 674, 378.
- Cho, J., and Lazarian, A., 2004, ApJ, 615, L41.
- Coronti, F. V., 1990, ApJ, **349**, 538.
- Dastgeer, S., Das, A., Kaw, P., and Diamond, P. H., 2000, Phys. Plasmas, 7, 571.
- Daughton, W., and Karimabadi, H., 2007, Phys. Plasmas, 14, 072303.
- Gary, S. P., 1993, *Theory of Space Plasma Microinstabilities*, Cambridge University Press, New York.
- Gary, S. P., and Borovsky, J. E., 2004, J. Geophys. Res., 109, A06105.
- Gary, S. P., and Borovsky, J. E., 2008, J. Geophys. Res., 113, A12104.
- Gary, S. P., and Karimabadi, H., 2009, Phys. Plasmas, 16, 042104.
- Gary, S. P., Saito, S., and Li, H., 2008, Geophys. Res. Lett., 35, L02104.
- Iwamoto, N. (1993), Phys. Rev. E, 47, 604.
- Kazimura, Y., Sakai, J. I., Neubert, T., and Bulanov, S. V., 1998, ApJ, 498, L183.
- Li, H., Gary, S. P., and Stawicki, O., 2001, Geophys. Res. Lett., 28, 1347.

- Marscher, A. P., Jorstad, S. G., Gomez, J. L., McHardy, I. M., Krichbaum, T. P., and Agudo, I., 2007, *ApJ*, 665, 232.
- Oughton, S., and Matthaeus, W. H., 2005, *Nonlinear Processes in Geophys.*, 12, 299.
- Ramirez-Ruiz, E., Nishikawa, K.-I., and Hededal, C. B., 2007, *ApJ*, 671, 1877.
- Saito, S., Gary, S. P., Li, H., and Narita, Y., 2008, *Phys. Plasmas*, 15, 102305.
- Swisdak, M., Liu, Y.-H., and Drake, J. F., 2008, *ApJ*, 680, 999.
- Yin, L., Daughton, W., Karimabadi, H., Albright, B. J., Bowers, K. J., and Margulies, J., 2008, *Phys. Rev. Lett.*, 101, 125001.

Fig. 1.— The linear damping rates of the Alfvén-like (dashed line) and magnetosonic-like (solid line) modes in electron-positron plasmas as functions of the angle of propagation relative to  $\mathbf{B}_o$ . Here  $\beta_e = 0.10$  and  $kc/\omega_e = 0.10$ .

Fig. 2.— The linear damping coefficient  $A(\beta_e)$  defined by Equation (2) for the Alfvén-like mode in electron-positron plasmas. Results here apply at least on the domain  $60^\circ \leq \theta \leq 85^\circ$ .

Fig. 3.— Linear theory results: The contours of  $\gamma/|\Omega_e| = 10^{-3}$  and  $10^{-2}$  for magnetosonic-like (solid lines) and Alfvén-like (dashed lines) fluctuations in electron-positron plasmas in  $k_\perp$  versus  $k_\parallel$  space. Here  $\beta_e = 0.10$ .

Fig. 4.— Linear theory results: The parallel dissipation wavenumber  $k_{\parallel d}$  for both Alfvén-like and magnetosonic-like fluctuations at  $k_\perp = 0$  as a function of  $\beta_e$  for  $\gamma/|\Omega_e| = -0.01$  and  $-0.001$ . The solid lines represent the scaling of the dissipation wavenumber with the electron inertial length, whereas the dashed lines represent  $k_{\parallel d}$  scaled with the electron gyroradius.

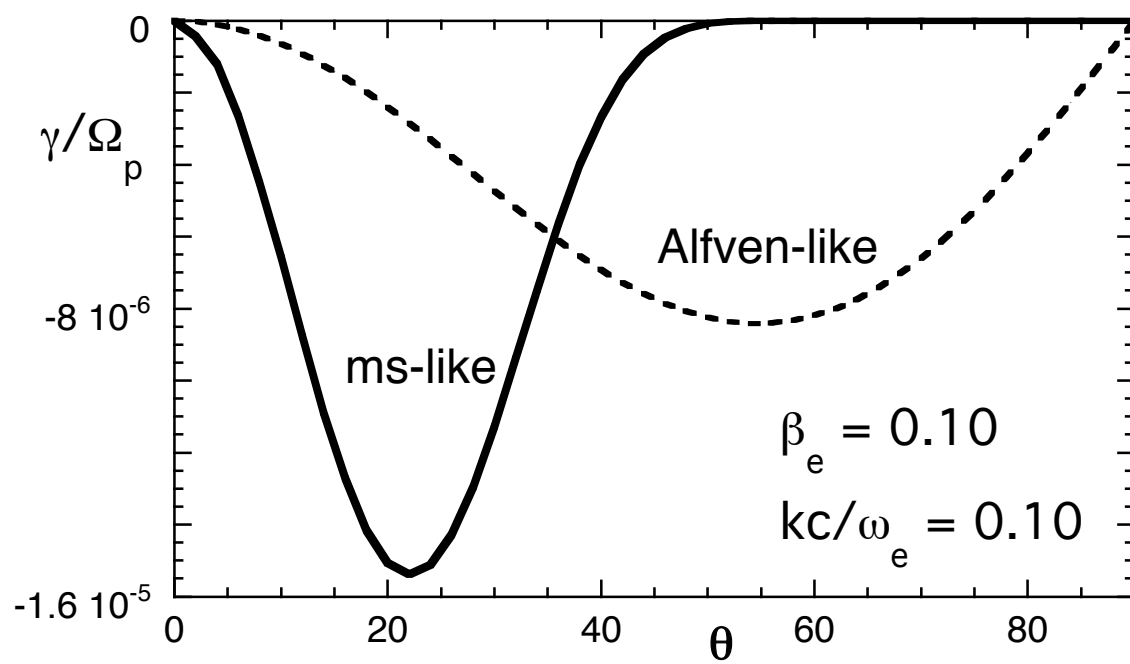


Figure 1

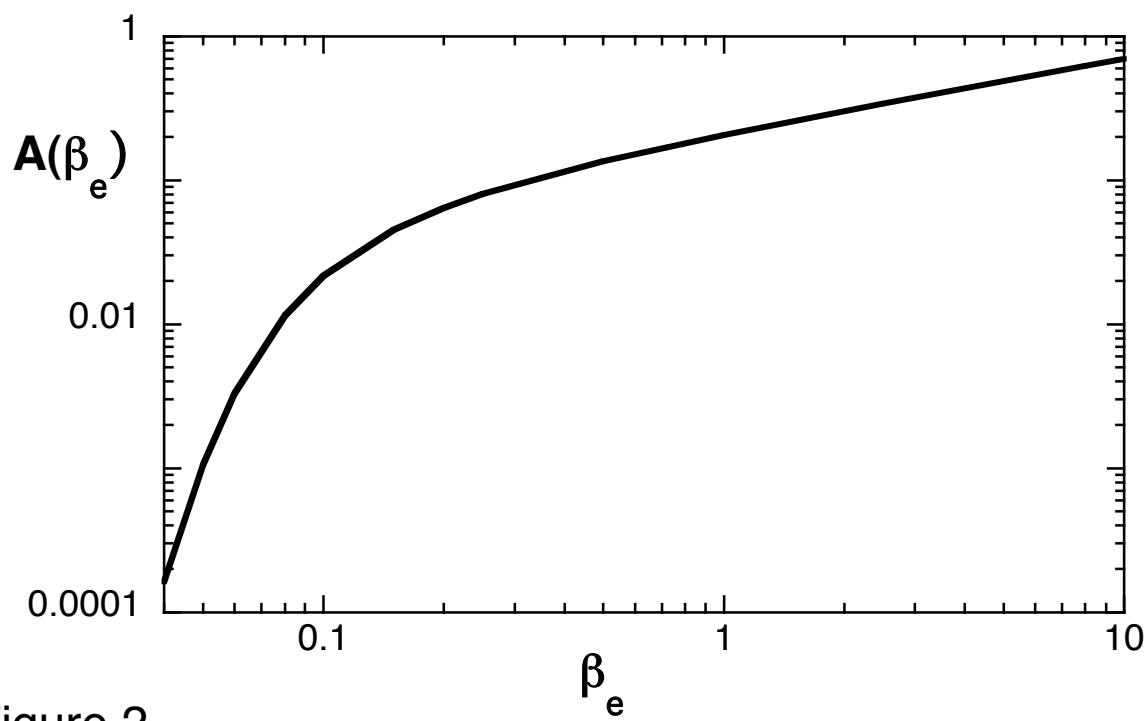
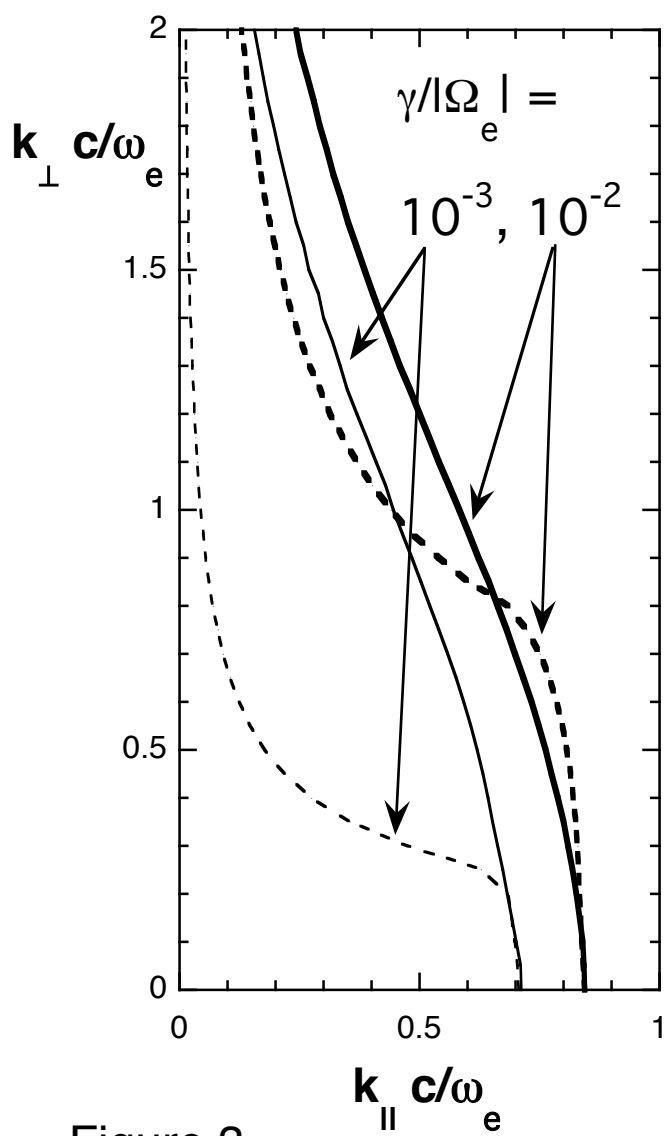


Figure 2



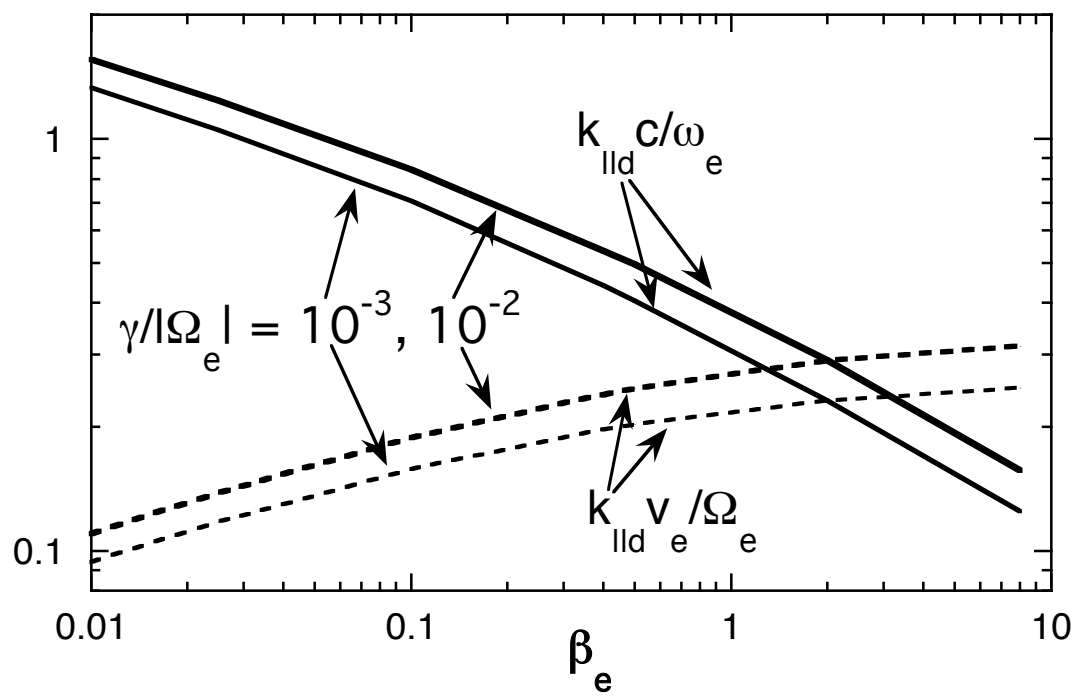


Figure 4